GEOLOGICA CARPATHICA, OCTOBER 2015, 66, 5, 393–407 doi: 10.1515/geoca-2015-0033

On the peritidal cycles and their diagenetic evolution in the Lower Jurassic carbonates of the Calcare Massiccio Formation (Central Apennines)

MARCO BRANDANO[1,2], LAURA CORDA[1], LAURA TOMASSETTI[1] and DAVIDE TESTA[1]

[1]Department of Earth Sciences, Sapienza University of Rome, P. Aldo Moro 5, I-00185, Italy;
laura.corda@uniroma1.it; laura.tomassetti@uniroma1.it; davidetesta.86@gmail.com
[2]Institute of Environmental Geology and Geoengineering (IGAG) CNR, Via Salaria km 29, I-00016, Italy; marco.brandano@uniroma1.it

(Manuscript received March 4, 2015; accepted in revised form June 23, 2015)

Abstract: This paper shows the environmental changes and high-frequency cyclicity recorded by Lower Jurassic shallow-water carbonates known as the Calcare Massiccio Formation which crop out in the central Apennines of Italy. Three types of sedimentary cycle bounded by subaerial erosion have been recognized: Type I consists of a shallowing upward cycle with oncoidal floatstones to rudstones passing gradationally up into peloidal packstone alternating with cryptoalgal laminites and often bounded by desiccation cracks and pisolitic-peloidal wackestones indicating a period of subaerial exposure. Type II shows a symmetrical trend in terms of facies arrangement with peloidal packstones and cryptoalgal laminites present both at the base and in the upper portion of the cycle, separated by oncoidal floatstones to rudstones. Type III displays a shallowing upward trend with an initial erosion surface overlain by oncoidal floatstones to rudstones that, in turn, are capped by pisolitic-peloidal wackestones and desiccation sheet cracks. Sheet cracks at the top of cycles formed during the initial phase of subaerial exposure were successively enlarged by dissolution during prolonged subaerial exposure. The following sea-level fall produced dissolution cavities in subtidal facies, while the successive sea-level rise resulted in the precipitation of marine cements in dissolution cavities. Spectral analysis revealed six peaks, five of which are consistent with orbital cycles. While a tectonic control cannot be disregarded, the main signal recorded by the sedimentary succession points toward a main control related to orbital forcing. High frequency sea-level fluctuations also controlled diagenetic processes.

Key words: cyclostratigraphy, diagenesis, Calcare Massiccio, Apennines, Jurassic.

Introduction

One goal of the sedimentologist is to decipher signals recorded in the sedimentary record. The carbonate sedimentologist has to understand how and where carbonate sediments have been created in response to intrinsic and extrinsic mechanisms forced by tectonic, eustatic, oceanographic and climatic processes, and ecological changes (Lukasik & Simo 2008; Strasser & Vedrine 2009; D'Argenio et al. 2011).

Modern carbonate platforms provide a means to examine how many depositional processes occur and demonstrate the complexity of facies associations (Wright & Burgess 2005; Strasser & Vedrine 2009). When dealing with carbonate platforms in the geological past, detecting facies associations and the origin of stacked cycles becomes more difficult. In particular, a long debated problem in stratigraphy is whether to relate the formation of peritidal carbonate cycles to autocyclic processes (Hardie 1986; Pratt et al. 1992) or to allocyclic processes (both Milankovitch and tectonic models). Autocyclic processes include progradation of shorelines and lateral migration of tidal channels, tidal inlets and bars (Ginsburg 1991). These processes are inherent to the shallowest environments of the platform (Strasser 1994). Cyclical perturbation of the Earth's orbit induces changes in the insolation and consequently sea level, climatic, oceanographic, sedimentary, and biological changes that are potentially recorded in the sedimentary archives through geological time (Strasser 1994; Strasser et al. 2006). In the case of proved Milankovitch cyclicity, the duration of the smaller-scale depositional sequences lies within the Milankovitch frequency band, then a very narrow time framework of 20, 41 and 100 to 400 ka can be established (Strasser et al. 1999, 2006; D'Argenio et al. 2011). Twenty-one ka cyclicity is produced by the precession of the equinoxes, 41 ka cyclicity is related to the obliquity of the Earth's axis, and the 100–400 ka cyclicity is produced by variation in the eccentricity of the ellipse of the Earth's orbit of ~100 (short eccentricity) and ~400 ka (long eccentricity) periods.

On the basis of stacking patterns and time-series analysis of western Mediterranean Lower Jurassic shallow-water carbonates, Crevello (1991) recognized a Milankovitch-type cyclicity. However, tectonic subsidence changes can also produce sedimentary cycles. Burgess (2001) showed that shoreline and island progradation, controlled by subsidence and sediment transport rate, are also plausible mechanisms to create variable thickness, shallowing-upward peritidal parasequences and should be considered in interpretations of such strata. Based on datasets from different Lower Jurassic peritidal cycles from western Tethyan platforms, Bosence et al. (2009) argued strongly for an overriding tectonic control on cycle formation.

This paper illustrates the high frequency cyclicity of the Lower Jurassic shallow-water carbonates known as the Calcare Massiccio Formation. The Calcare Massiccio Formation belongs to the Tethyan Liassic carbonate platform domain that developed in the large epicontinental sea that covered shelf areas of present-day North Africa and Western Europe as well as the Apennines and the Pelagonian platform of present-day Greece (Bosence et al. 2009). In the Apennines, the Calcare Massiccio Formation is characterized by lateral variation in depositional environments and in thickness, probably related to an articulated physiography of the Triassic to Lower Jurassic carbonate platform (Centamore et al. 1971). For this reason, it has been subdivided into a number of lithostratigraphic sub-units. The articulated physiography was attributed to the beginning of tectonic extension, which created two different domains: a persistent carbonate platform (Latium-Abruzzi domain) and a deep-water domain (Umbria-Sabina Basin) with intrabasinal structural highs. On the structural highs, the Calcare Massiccio Formation is characterized by peritidal cyclical sedimentation and is usually overlain by pelagic sea-mount deposits represented by condensed pelagic cephalopod-rich carbonates of the upper Pliensbachian–Tithonian Bugarone unit (reduced sequences) that are no more than a few tens of metres thick (Centamore et al. 1971; Pialli 1971; Colacicchi et al. 1975). Deposition in the structural depressions was characterized by the relatively deep, subtidal Calcare Massiccio Formation that does not show evidence for cyclical sedimentation (Santantonio 1993).

Notwithstanding the great extent of the Tethyan Liassic carbonate platform, few works have analysed the origin of the sedimentary cyclicity following a cyclostratigraphic approach (Bigozzi 1990; Bosence et al. 2000, 2009). This approach uses astronomical cycles of known periodicities to date and interpret the sedimentary record (Strasser et al. 2006).

This paper presents an analysis of environmental and diagenetic changes recorded in the Calcare Massiccio Formation deposited on structural highs. Based on detailed logging and facies analysis of a well exposed section, sedimentary cycles are defined according to cyclostratigraphic concepts. This paper aims to distinguish the controlling factors producing the cyclicity of the Calcare Massiccio Formation, and to evaluate the role of autocyclic vs. allocyclic processes.

Geological setting

The studied area is located near S. Angelo Romano village, in the Cornicolani Mountains (Fig. 1b). These mountains belong to the Apennine chain and represent a structural high within the Sabina Basin that developed from the Pliensbachian to Tithonian.

The Apennines are an asymmetric fold and thrust belt developed on top of an eastward-retreating westward dipping continental slab attached to the Adriatic plate (Doglioni 1991; Carminati & Doglioni 2005; Carminati et al. 2010, 2013). The Neogene to Quaternary evolution of the Northern-Central Apennines is characterized by east-north-eastward migration of deformation fronts of the related foredeeps coupled with extensional tectonics in the hinterland leading to the opening of progressively younger backarc basins (Gueguen et al. 1998).

The central Apennines fold-and-thrust belt consists of a Meso-Cenozoic succession deposited on the Adria passive margin (Fig. 1a). Deposition began with continental to marine clastic sediments followed first by Upper Triassic dolomitic and/or evaporitic deposits (Burano Formation) and then by Lower Jurassic peritidal carbonates represented by the Calcare Massiccio Formation, which ranges in thickness from three to seven hundred meters (Pialli 1971). The Calcare Massiccio Formation is generally dated Late Hettangian–Early Pliensbachian (*Ibex* Biozone). Deposition of peritidal carbonate sediments persisted from Late Hettangian to Sinemurian when a rifting phase led to platform fragmentation and drowning. The resulting complex architecture was characterized by spatial and temporal variations in subsidence rates (Carminati et al. 2013), produced by extensional tectonic processes, which created a persistent carbonate platform (Latium-Abruzzi carbonate platform), a deep-water domain (Umbria-Marche and Sabina pelagic basin) and intrabasinal morpho-structural highs (Centamore et al. 1971; Damiani et al. 1992; Santantonio 1993; Galluzzo & Santantonio 2002; Cosentino et al. 2004).

From the Sinemurian onward, the Latium-Abruzzi carbonate platform persisted as a monotonous repetition of subtidal and peritidal cycles, interrupted by short periods of emersion, which were associated with bauxite development. After the fragmentation and drowning of the Hettangian-Sinemurian platform, the Umbria-Marche and Sabina domain developed into a wide pelagic basin with scattered fault-bounded structural highs (pelagic carbonate platforms *sensu* Santantonio 1993) characterized by normal and condensed pelagic deposits, respectively. The structural-high blocks, within the Umbria-Marche and Sabina domain were characterized by high subsidence rates occurring during the deposition of the Calcare Massiccio Formation (Carminati et al. 2013). With the activation of late Hettangian–Sinemurian extensional tectonics, subsidence rates drastically increased in the sectors which would later host thick pelagic successions (the definitive drowning of the Calcare Massiccio platform occurred in the Early Sinemurian). At the structural highs, the shallow-water deposition of the Calcare Massiccio Formation persisted until the Sinemurian–Early Pliensbachian and was followed by condensed pelagic deposits (Santantonio 1993; Passeri & Venturi 2005).

Analysis of sedimentary cycles in the Calcare Massiccio Formation was first undertaken by Colacicchi et al. (1975). These authors recognized sequences of facies evolving gradually from subtidal to supratidal environments arranged into predominantly shallowing upward cycles. The authors also reported the occurrence of cycles, which do not follow this Waltherian model, but document the superposition of supratidal facies directly on subtidal facies. The same cycles were also recognized by Bigozzi (1990) who showed an organized stacking pattern consisting of megacycles each comprising five individual cycles and interpreted as the product of high-frequency sea-level changes probably produced by variation of orbital parameters. Successively, Bosence et al. (2009)

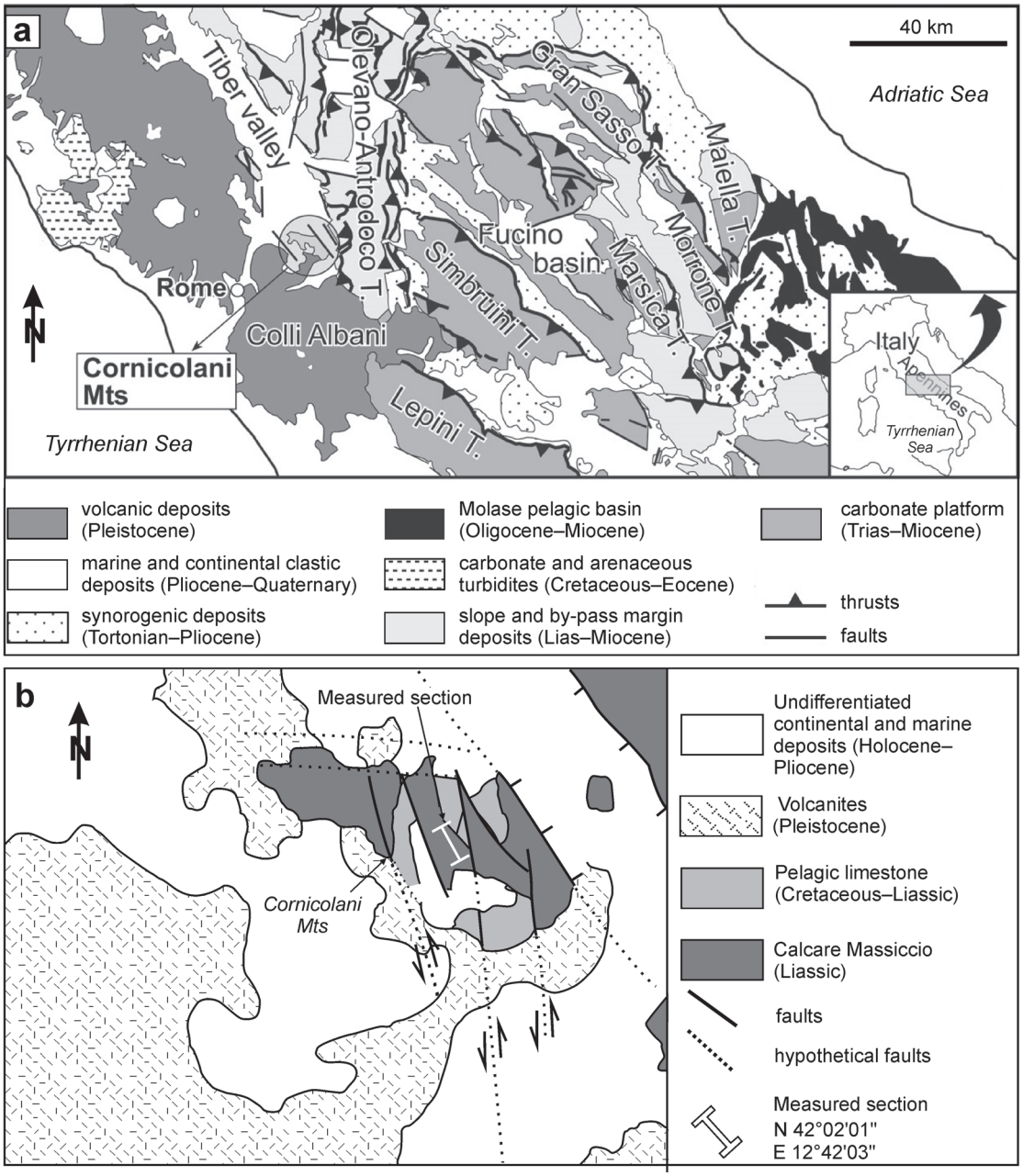

Fig. 1. Geological situation, from general to detail. **a** — schematic geological map of Central Apennines, **b** — geological map of Cornicolani Mountains and location of studied section (modified from Billi et al. 2007).

presented the analysis of different Lower Jurassic successions along the Tethys margin including the Apennines succession in Umbria. These authors recognized five sedimentary cycles, two of them present in the Umbrian Apennines succession (α and γ). According to Bosence et al. (2009), α cycles are asymmetrical, shallowing-upward cycles that evolve upward from open-marine to subaerial or restricted marine to intertidal facies associations. Cycle boundaries are marked by erosional surfaces overlain by evidence of marine flooding. The γ cycles show a symmetrical arrangement of facies with a transgressive phase, an interval of maximum marine flooding, followed by a regressive phase capped by an erosional surface. In these cycles, the intertidal and subaerial facies associations are well developed and the top of the cycle is characterized by calcretes with tepees. According to Bosence et al. (2009), both α and γ cycles may be generated by allocyclic and autocyclic mechanisms. The other three cycle types characterizing the Liassic platform outside the Apenninic domain are: the deepening upward β cycles bounded by an erosional surface; the asymmetrical δ cycles composed of subtidal sedimentary facies with a subaerial diagenetic overprint affecting its upper surface; the ε cycles, which are characterized by subtidal facies with a deepening upward trend. According to Bosence et al. (2009), these cycles can be generated only by allocyclic controls. The common character of these cycles is the scarcity of intertidal facies, dominance of subtidal facies

and a deepening upward trend indicative of relatively more open marine environments.

The investigated stratigraphic section comes from the end of the upper portion of the Calcare Massiccio Formation cropping out in the Cornicolani Mountains. Many sedimentological works on the Calcare Massiccio demonstrate a cyclically monotonous alternation of few lithofacies forming α and γ cycles (sensu Bosence et al. 2009), although the formation displays a remarkable thickness of up to 700 m (Pialli 1971; Colacicchi et al. 1975; Bigozzi 1990; Barattolo & Bigozzi 1996; Passeri & Venturi 2005; Bosence et al. 2009). In this work, we present a high-resolution analysis of a very well exposed road cutting (26 m exposed thickness) located in the structural high of the Cornicolani Mountains at the end of the upper portion of the Calcare Massiccio Formation, around 40 m before the drowning succession. Notwithstanding the limited thickness, this section displays facies associations typical of the peritidal cycles characterizing the Calcare Massiccio and can be considered representative of the recorded cyclicity.

Material and methods

An outcrop in an abandoned quarry and a well-exposed stratigraphic section along the road to S. Angelo Romano village provide a good opportunity to study the facies associations of Calcare Massiccio Formation (Fig. 1). Textural and compositional data were observed in the field at centimeter scale, providing a virtually continuous sedimentological data set recording the stratigraphic evolution of the investigated interval. For the sedimentary cycle identification we followed the methodology of Bosence et al. (2009). We used the term sedimentary cycle to identify commonly repeated meter-scale lithofacies successions. These cycles comprise bundles of beds of different thickness separated by erosional surfaces. Each erosional surface is overlain by relatively open marine facies (e.g. subtidal facies) evolving upward to shallower more restricted facies (from intertidal to supratidal facies). The cycle boundary is placed at the most prominent erosional surface or at a non-Waltherian facies shift at the accommodation minima, for example, at the subtidal facies directly overlying a subaerial exposure surface, or intertidal facies.

In order to better characterize the sedimentary facies and the composition of the investigated carbonates, 82 samples were collected along the measured section (Fig. 2). A selected set of 70 thin sections was studied and classified according to the nomenclature of Dunham (1962) and Embry & Klovan (1971) for carbonate rocks and their compositional and diagenetic characteristics recorded. Ten selected thin sections were polished and examined under cathodoluminescence (CL) microscopy at the Earth Science Department "Ardito Desio" of the University of Milan. Twenty selected thin sections, were polished and carbon-coated and subjected to electron microprobe analysis to determine the concentration of Mg, Sr, Mn, Fe and Ba (CAMECA instrument — Istituto di Geologia Ambientale e Geoingegneria-CNR, University of Roma "La Sapienza").

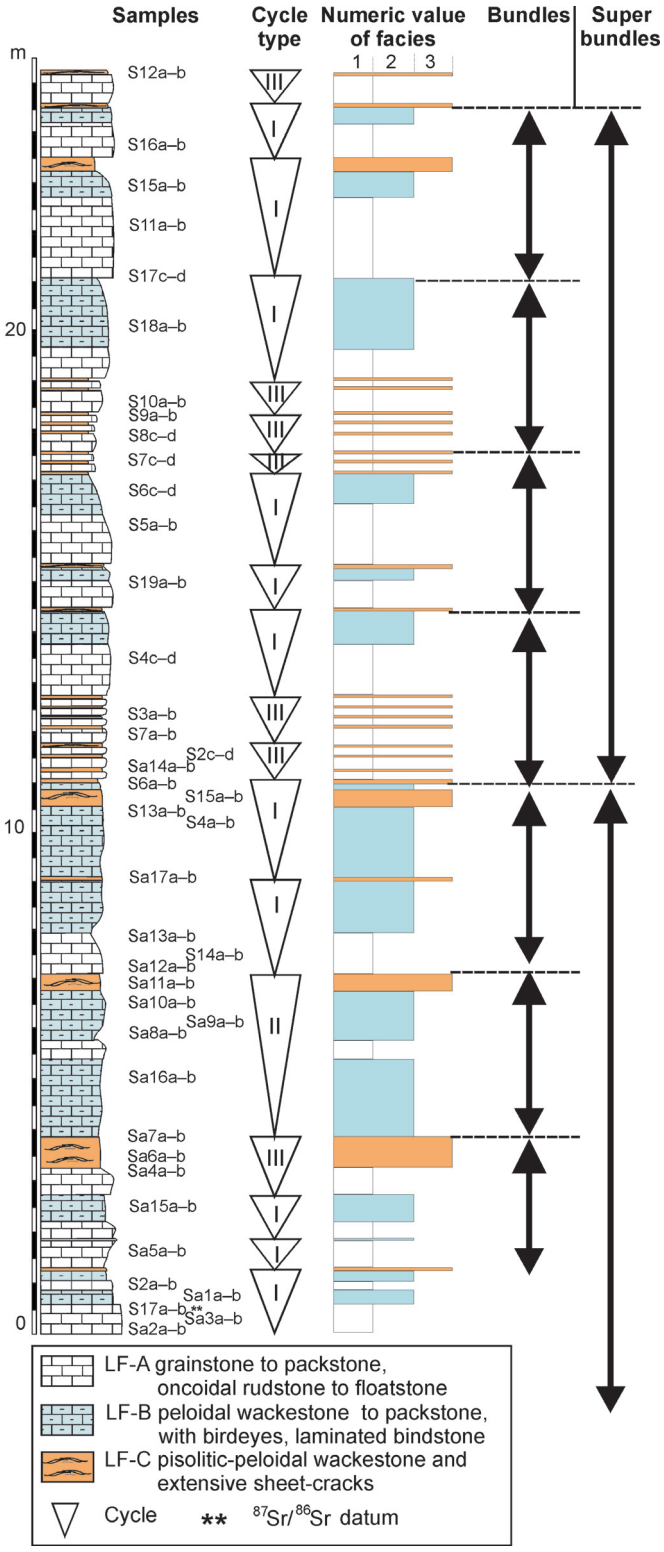

Fig. 2. Measured section from the Calcare Massiccio Formation and thickness recurrences of the main facies associations.

Twenty oxygen and carbon stable isotope analyses were carried out on 15 samples obtained with a hand-operated microdrill, using 0.5 mm Ø tungsten drill bits. All of the different recognized cements were sampled. Analyses were per-

formed using a Finnigan MAT 252 mass spectrometer at the isotope geochemistry laboratory of the Istituto di Geologia Ambientale e Geoingegneria-CNR. The results were calibrated using NBS carbonate standard and are reported on the PeeDee belemnite (PDB) scale. The analytical precision for the isotope data is ±0.1 ‰ based on replicate standards.

$^{87}Sr/^{86}Sr$ dating was carried on the micrite of pure lime-mudstones. It was microdrilled after examination under cathodoluminescence with the luminescent portion being discarded. Isotopic analyses were performed at IGAG-CNR (Dipartimento di Scienze della Terra, University of Rome "La Sapienza") using a Finnigan MAT 262RPQ multi-collector mass spectrometer. All samples were loaded on a double Re filament as nitrate and analysed in static mode. Measured Sr isotope ratios were normalized for mass fractionation to $^{87}Sr/^{86}Sr = 0.1194$. NBS987 yielded a $^{86}Sr/^{87}Sr$ value of 0.710235+/–10. The averaged analytical error (2σ) of $^{86}Sr/^{87}Sr$ was ±0.000011 (n = 16). The $^{86}Sr/^{87}Sr$ values of the samples were converted to numerical ages using Version 4B: 08/04 of the Look-Up Table of Howarth & McArthur (1997).

An observational time series was generated from the measured stratigraphic section. A numerical value (1–3) was assigned to each facies association recognized (Fig. 2). A spot sampling method was used to generate continuous-signal records (Weedon 2003). The classical method of searching for cyclicity in time series uses spectral analysis. This method looks at time series in terms of their frequency composition (Schwarzacher 1993). Time-series analysis of the investigated section was performed by using thickness recurrences of the main facies associations (Fig. 2). The sampling interval to perform the time series analysis was 1 cm, which was chosen based on the facies-thickness data for the investigated section. To mathematically study the signal frequency, Fourier analysis was performed with the Macintosh-based software Analyseries 1.1 (Paillard et al. 1996). The maximum entropy approach and the Blackman-Tuckey power spectrum estimator were used (Blackman & Tuckey 1958).

Results

In the studied section, three lithofacies associations (LF-A, -B, and -C) were identified based on texture, main constituents, fabrics and early diagenetic features. These are interpreted as representing the three main sedimentary environments of the inner platform environment represented by the Calcare Massiccio Formation (Table 1). According to the studies on modern and ancient peritidal carbonate systems (Pratt et al. 1992; Strasser & Vedrine 2009), the sedimentological interpretation leads to a facies model representing the spatial distribution of the products of different sedimentary processes occurring in the different environments of the Calcare Massiccio platform.

The investigated section comprises the last interval of the Calcare Massiccio Formation in the Cornicolani Mountains, where outcrops occur of about a hundred meters of peritidal carbonates covered by beds of the drowing succession (Cosentino et al. 2004).

The isotopic age obtained from strontium isotope analysis of micrites from the base of the section (Fig. 2) approximates 194.30 Ma confirming a Sinemurian age for the upper part of the formation. Lastly 19 sedimentary cycles have been recognized, with thickness ranging between 0.5 and 3 m, with average of 1.36 m.

Lithofacies associations

LF-A packstones to grainstones with ooids, oncoidal floatstones to rudstones

This facies association is characterized by two sublithofacies: packstones to grainstones (LF-A1) and oncoidal floatstone to rudstone (LF-A2). LF-A1 comprises abundant ooids, peloids (fecal pellets, algal peloids, microbial peloids) and aggregate grains such as lumps. The ooids show a large micritized nucleus and a very thin cortex characteristic of superficial ooids (*sensu* Carozzi 1957). Typical skeletal grains are small benthic foraminifera (valvulinids, textulariids and lituolids), ostracods, mollusc fragments and cortoids, small ammonites, *Cayeuxia*, thaumatoporellids, and porostromata cyanobacteria (Fig. 3a). LF-A2 is dominated by oncoids of various shape and size (up to 2 cm). Two types of oncoids are identified: Type 1 and Type 2 (*sensu* Védrine et al. 2007). Type 1 oncoids are up to 0.5 mm in diameter and show spherical to elliptical shape with smooth contours. The cortex is micritic, homogeneous and lacks associated microencrusting

Table 1: Lithofacies associations of the Calcare Massiccio Formation and their interpreted environmental setting.

Lithofacies associations	Sub-lithofacies	Components	Environment
LF-A packstones to grainstones with ooids, oncoidal floatstones to rudstones	Packstones to grainstones (LF-A1)	Peloids, superficial ooids, lumps and subordinate small benthic foraminifera, ostracods, mollusc fragments, cortoids, *Cayeuxia*, thaumatoporellids, porostromata cyanobacteria	Shallow subtidal environment under moderately to high energy conditions characterizing lagoonal channels or shoals
	Floatstones to rudstones (LF-A2)	Type 1 and type 2 oncoids, matrix comprising peloids and skeletal fragments	
LF-B peloidal wackestones to packstones alternating with cryptalgal bindstone	Peloidal wackestones to packstones (LF-B1)	Peloids, small benthic foraminifera lituolids and textulariids, small ostracods, serpulids, gastropod fragments and *Cayeuxia*	Intertidal and supratidal environment
	Bindstones (LF-B2)	Planar algal laminae and trapped mud, type 3 oncoids with *Bacinella irregularis*, *Lithocodium aggregatum*, *Cayeuxia*, subordinate type 2 oncoids	
LF-C pisolitic-peloidal wackestones with extensive sheet-cracks		Pisoids and peloids	Supratidal environment

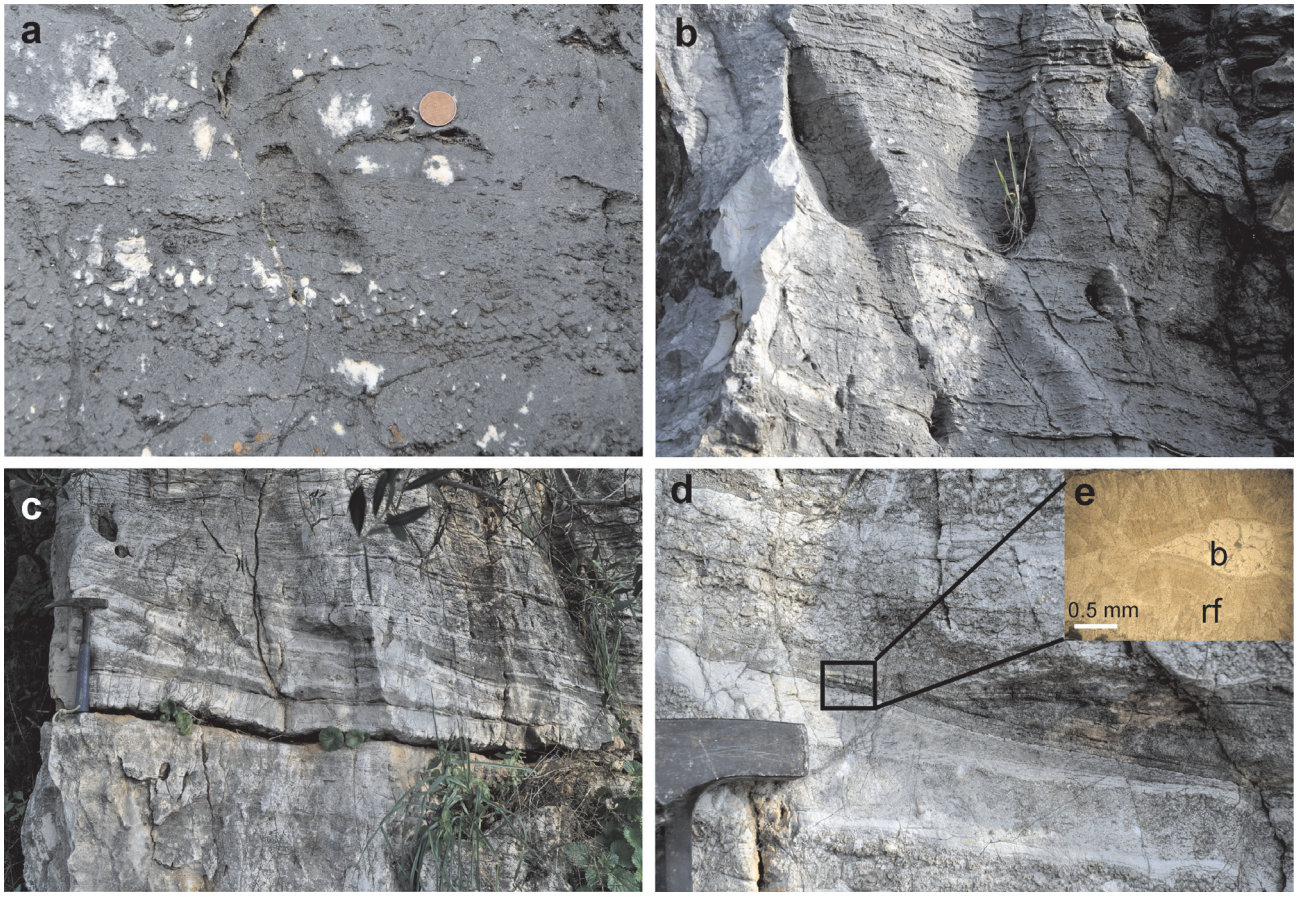

Fig. 3. Field photographs of the recognized lithofacies associations. **a** — LF-A packstone to grainstone with ooids, oncoidal floatstone to rudstone that forms decimetric thick beds; **b** — LF-B peloidal wackestone to packstone with birdeyes and laminated bindstone; **c** — LF-C pisolitic-peloidal wackestone alternating with extensive sheet-cracks; **d** — detail of sheet cracks overlaid by oncoidal rudstone; **e** — photomicrograph of sheet cracks with isopachous radiaxal fibrous cement (rf) followed by blocky cement (b).

fauna. Laminations are micritic but rarely visible. Nuclei are lithoclastic and comprise small ooids and/or aggregate grains. Type 2 oncoids have diameters of between a few millimeters and 2 cm and elliptical to elongated shapes with smooth contours. The cortex is micritic with laminae easily recognizable. Laminae are micritic but irregular and locally truncated, showing different growth phases. Couplets of micritic and sparry laminae are present and accentuate the laminar structure of the Type 2 oncoids. Both lithoclastic (peloids, ooids) and bioclastic (echinoid fragments, *Cayeuxia*) nuclei occur (Fig. 4a). Occasionally, small ooids are incorporated into the cortex. Some serpulids and small articulated ostracods also occur within the matrix.

The matrix of the oncoidal floatstones to rudstones consists of fine-grained peloids or skeletal fragments. When the matrix is lacking, oncoids are usually surrounded by a thin rim of isopachous fibrous cement and later drusy mosaic cement. Dissolution cavities are diffuse and infilled by drusy mosaic cement (Fig. 5a).

Interpretation:

This facies association was deposited in a shallow subtidal environment under moderate to high energy conditions characterizing lagoonal channels or shoals (Colacicchi et al. 1975; Barattolo & Bigozzi 1996; Pomoni-Papaioannou & Kostopoulou 2008) as demonstrated by the textural charac-

Fig. 4. Photomicrographs of the lithofacies associations. **a** — LF-A, oncoidal rudstone, dominated by Type 2 oncoids; **b** — LF-B, cryptalgal bindstone consisting of micritic laminae (black arrows) produced by microbial mat, fine grained laminated peloidal packstone to grainstone passing into peloidal wackestone and fenestral cavities (white arrow); **c** — LF-C, laminated crust, composed of radiaxial fibrous cement and thin micritic laminae. Note the articulated ostracod concentration (black arrow); **d** — type 2 oncoids with Cayeuxia nuclei, and isopachous fibrous cement around the oncoids; **e** — dissolution cavity with a fibrous cement rim and drusy mosaic cement in the central portion; **f** — detail of the crust of fibrous cement consisting of two or more growth zones of cloudy fibrous crystals a few millimeters in size (black arrow), growing perpendicularly to the substrate; **g** — detail of drusy mosaic cement; **h** — this drusy cement under cathodoluminescence is alternating bright and non-luminescent.

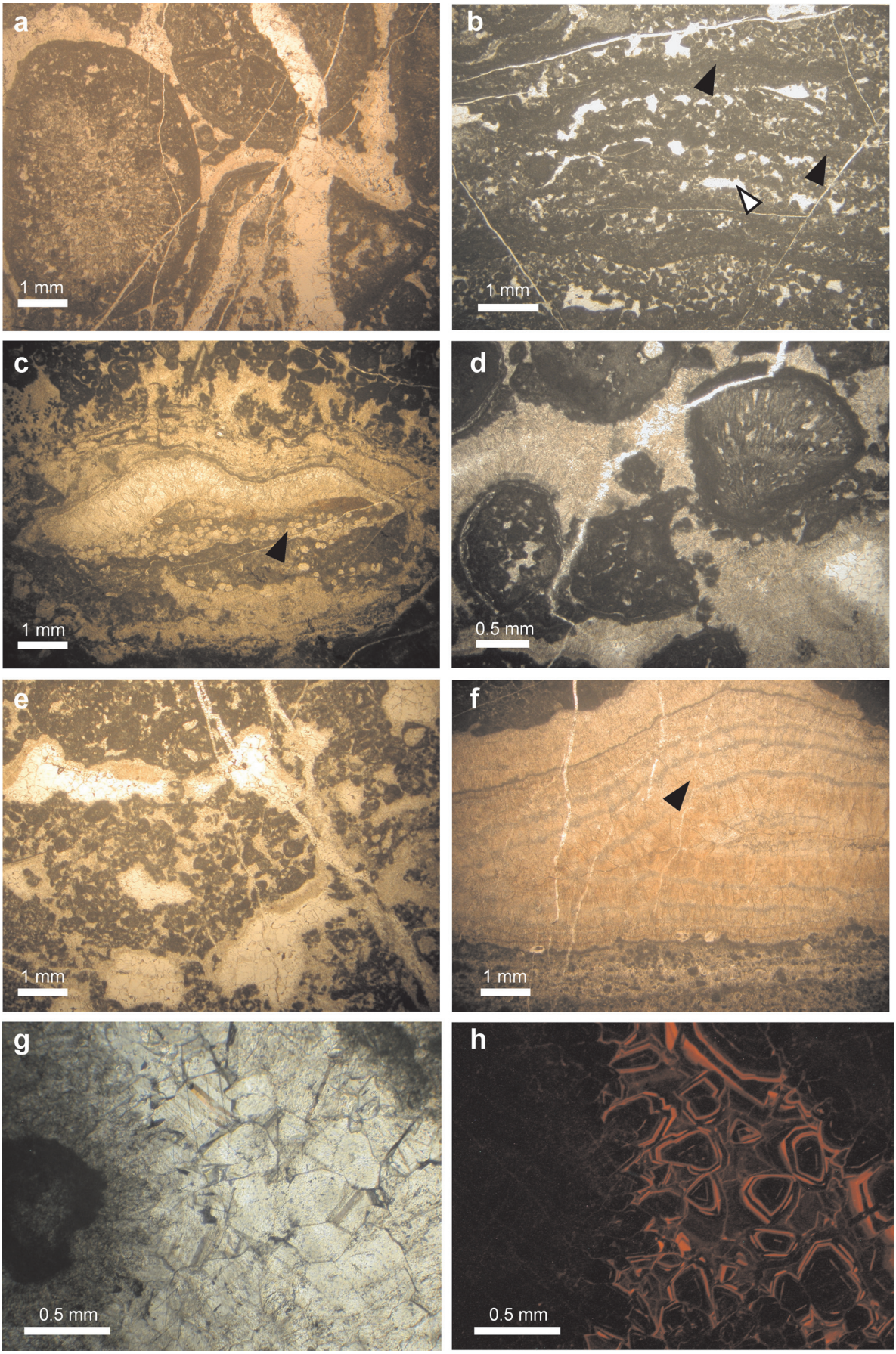
a
1 mm
b
1 mm
c
1 mm
d
0.5 mm
e
1 mm
f
1 mm
g
0.5 mm
h
0.5 mm

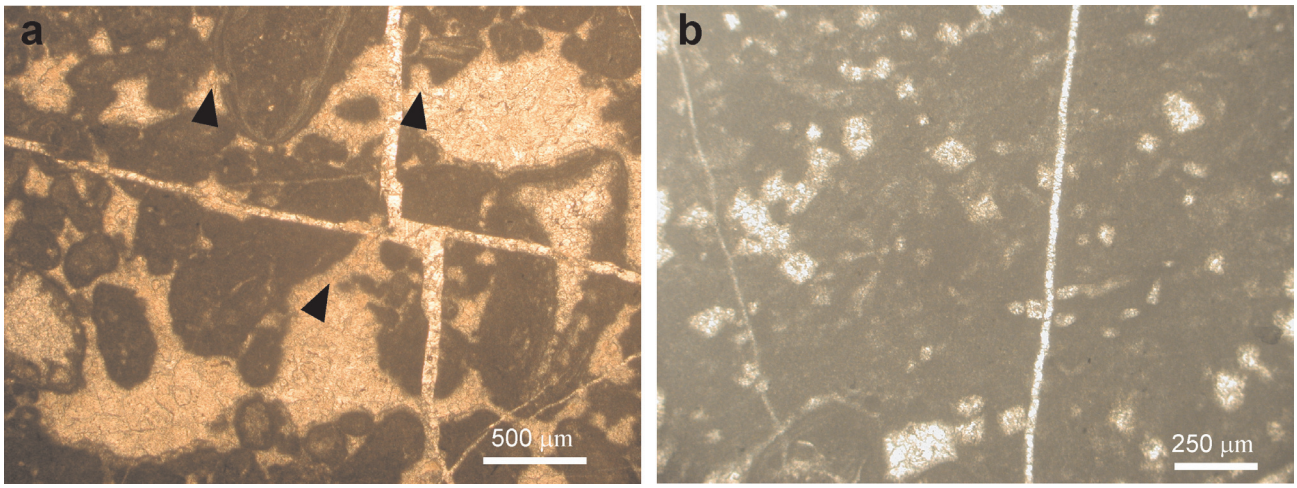

Fig. 5. a — dissolution cavity with fibrous cements, black arrows show leached grains, solution enlarged pores; **b** — isolated euhedral planar crystals of dolomite within the fine grained matrix interval of LF-B and LF-C facies associations.

teristics. Shallow water, high energy conditions are also supported by the presence of oncoids that were able to overturn and roll (cf. Védrine et al. 2007) as demonstrated by their sub-spherical to elliptical shape.

LF-B peloidal wackestones to packstones alternating with cryptalgal bindstone

This facies association comprises two sublithofacies: (i) peloidal wackestones to packstones (LF-B1) alternating with (ii) cryptalgal bindstone with birdseyes and fenestral fabrics (LF-B2) (Figs. 3b and 4b). Geopetal structures and irregularly shaped peloidal-micritic intraclasts, derived from underlying lithologies, were also recognized.

Fenestrae are usually filled with drusy calcite; in some cases large irregular stromatactoid voids filled with fine-grained sediment are also recognizable. Peloids are up to 500 μm in diameter and equal-sized and they are associated with small benthic foraminifera lituolids and textulariids, small ostracods, serpulids, gastropod fragments and *Cayeuxia*. Gastropods and ostracods are often recrystallized and articulated ostracods may be preserved in the center of cavities filled with radial fibrous calcite.

Bindstones (LF-B2) are composed of stromatolitic layers, planar algal laminae and trapped mud (Fig. 4b). Couplets of micritic and clotted peloidal layers occur. This facies association is characterized by Type 3 oncoids (*sensu* Védrine et al. 2007). These oncoids are between 0.5 mm and 3 cm in diameter and show a sub-elliptical to lobate shape with wavy and

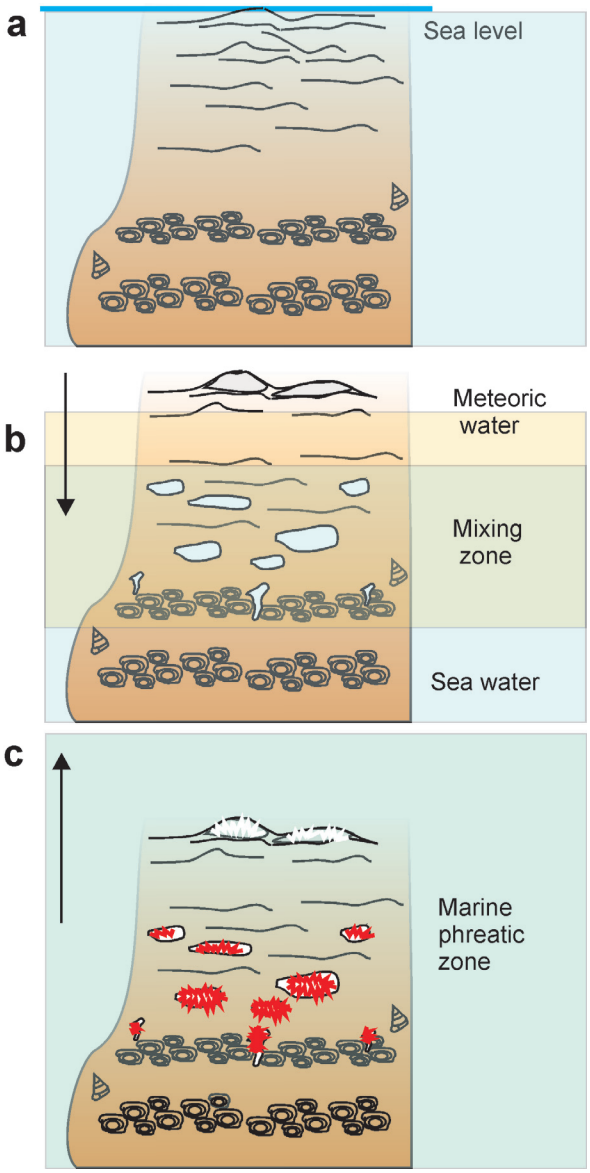

Fig. 6. Sketch illustrating the diagenetic imprint after the deposition of the sedimentary cycle of Calcare Massiccio. **a** — sheet cracks formed during initial subaerial exposure are successively enlarged by dissolution during prolonged subaerial exposure; **b** — the sea-level fall results in the enlargement of the meteoric zone and the lowering of the mixing zone producing dissolution cavities; **c** — sea-level rise produced the space for the accumulation of the overlying sedimentary cycle and precipitation of marine cement in the dissolution cavities.

irregular contours. The cortex comprises an alternation of organism-bearing and subordinate micritic laminae. Micritic laminae are rarely continuous. The organism-bearing laminae are predominant and comprise the microencrusting organisms *Bacinella irregularis* (Radoičić, 1959) and *Lithocodium aggregatum* (Elliott, 1956). *Bacinella* and *Lithocodium* are commonly assumed to be cyanobacterial organisms characterized by an irregular microbial meshwork, alveoli and interspaces filled with microsparry calcite (Schmid & Leinfelder 1996; Duprax & Strasser 1999). Oncoid nuclei are mainly bioclastic, made of echinoid or *Cayeuxia* fragments and gastropods, but also include small peloids or aggregate grains. Occasionally, small Type 2 oncoids with a *Bacinella–Lithocodium* envelope occur.

Micritic layers in this facies may show partial dolomitization with dolomite forming clear euhedral rhombs (Fig. 5b).

Interpretation:

This facies association is interpreted as the deposits of intertidal and supratidal environments. A characteristic feature of peritidal carbonates are millimeter-scale microbial laminated sediments commonly associated with fenestral and birdseye fabrics (Tucker & Wright 1990). Their preservation is most common in the upper intertidal zone as they are frequently disrupted by bioturbation in subtidal and lower intertidal environments.

Type 3 oncoids indicate relatively low-energy conditions characterized by *Bacinella–Lithocodium*. In fact, these microencrusters dominate in low to very low energy settings where the microbial meshwork had time to grow (cf. Védrine et al. 2007).

LF-C pisolitic-peloidal wackestones with extensive sheet-cracks

This facies association consists of barren mudstones to wackestones, which are locally dolomitized. The only fauna preserved are articulated ostracods (Fig. 4c). These deposits are characterized by the presence of sheet-cracks and laminoid-irregular fenestrae. The sheet-cracks can be laterally continuous on a decimeter to meter scale and are lined by an isopachous rim followed by coarse blocky calcite (Fig. 3c,d,e). Sheet-cracks consist of radiaxial fibrous calcitic cement with a horizontal or undulating trend (Figs. 3d and 4c). The cracks are up to 3 cm thick and occur individually or in stacked sets.

The sheet-cracks may be superimposed on the facies of LF-A and LF-B. They are often associated with pisolitic wackestones. Pisoids are centimeter-sized grains (up to 3 cm)

Table 2: Summary of the geochemical and isotopic data of the recognized cements.

Cement	Mn (ppm)	Fe (ppm)	Sr (ppm)	Ba (ppm)	Mg (ppm)	$\delta^{18}O$ ‰	$\delta^{13}C$ ‰
Isopachous fibrous	224	70	693	331	3023	–0.9	2.08
	418	241	481	188	2927	–0.80	2.03
	255	404	549	0	3074	–1.3	1.7
	224	0	211	376	2244		
	464	0	33	232	2960		
	0	310	515	0	2432		
	85	0	515	277	2089		
	464	0	67	420	2698		
Drusy mosaic	224	326	0	0	2206	–1.32	1.17
	0	0	0	0	2273	–1.87	1.11
	139	0	169	0	1197	–1	1.01
	0	139	279	0	2764		
	673	295.4	0	0	2106		
Blocky	0	0	177	0	2404	–3.97	0.34
	263	0	33.8	0	2529	–3.45	1.01
	0	0	0	0	1400	–3.8	0.8
	0	0	0	0	1616		
Radiaxial fibrous	464	0	67	420	2692	–2.21	2.25
	0	178	0	1200	1357	–1.15	2.5
	309	101	0	653	1993	–0.35	3.42
	0	264	0	850	2495	–0.53	3.02
	54	0	254	770	2931	–1.74	2.75
	170	124	346	609	1000	–1.2	1.6
	0	139	169	806	1411	–1.15	0.3
	0	178	0	797	1009	–1.02	1
	278	363	0	698	2479	–0.80	1.6
	0	101	0	609	2395	–1.02	2.8
Dolomite	0	0	0	0	43600		
	0	0	0	0	110340		
	0	0	0	0	80000		
	0	0	0	0	103430		
	0	0	0	0	94000		
	0	0	0	0	125780		
	0	0	0	0	116000		
	0	0	0	0	108750		
	0	0	0	0	60050		

with a concentric laminated structure. Nuclei are mainly small peloids and aggregate grains. Laminae are made of an alternation of thin micritic laminae and calcitic microspar. Some pisoids are fractured and fragmented. Peloidal bands with oxidized iron staining and some root-related structures also occur.

Some laminae are heavily disrupted by bioerosion traces.

Interpretation:

This facies association is interpreted as deposits from a supratidal environment. The interpretation is based on the abundance of laminar sheet cracks and features related to subaerial diagenesis, such as vadose pisolites, diffuse reddish iron oxides testifying extended periods of exposure, and partial dolomitization.

Diagenetic features

Four main types of calcitic cement were recognized in the analysed rocks: 1) isopachous fibrous cement on oncoids and bioclasts; 2) drusy mosaic cement infilling intergranular pores and dissolution cavities; 3) crusts of radiaxial fibrous cement constituting the sheet cracks; 4) blocky cement occluding large pores between the crusts of sheet cracks. The diagenetic feature includes also the presence of dolomite that occurs as matrix-dolomite.

The isopachous fibrous cement consists of closely packed crystals (10×70 μm) and occurs in interparticle and vuggy pores (*sensu* Choquette & Pray 1970), and in dissolution cavities (Figs. 4d, 5a). This cement is non-luminescent under cathodoluminescence (CL), is non ferroan-to slighty ferroan, with moderate Sr, Mn and Mg concentrations. Stable isotope values of this cement are around –0.90 ‰ for $\delta^{18}O$, and between +2.80 ‰ and +1.70 ‰ for $\delta^{13}C$.

The drusy mosaic cement developed mainly in interparticle and vuggy pores, and subordinately in intraparticle pores. It is characterized by a mosaic of polygonal, anhedral crystals ranging in size between 50 μm and 250 μm (Fig. 4e). Under CL, it comprises alternating bright and non-luminescent bands (Fig. 4g,h), with moderate Fe, Mn and Sr concentrations (Table 1). Stable isotope values are around –1.00 ‰ for $\delta^{18}O$ and +1.00 ‰ for $\delta^{13}C$.

The crusts of radiaxial fibrous cement consist of two or more growth zones of cloudy fibrous crystals 3–4 mm in length, growing orthogonal to the substrate and showing undulose extinction (Fig. 4f). This cement does not exhibit luminescence under CL. It is non-ferroan and Mg concentrations vary between 1300 and 2900 ppm. This cement is characterized by a Ba content of up to 1200 ppm. Stable isotope values range between –0.35 ‰ and –2.20 ‰ for $\delta^{18}O$ and +0.30 ‰ and +3.40 ‰ for $\delta^{13}C$.

The blocky cement is found in large pores between crusts of radiaxial fibrous cement in the sheet cracks. This cement is characterized by subhedral to anhedral crystals ranging from 0.2 to 1 mm in size. This cement is not luminescent under CL and is non-ferroan with moderate Mg concentrations (between 2100 and 2400 ppm). Stable isotope values range from –3.45 ‰ to –4.00 ‰ for $\delta^{18}O$ and from +0.34 ‰ to +1.10 ‰ for $\delta^{13}C$ (Table 2).

Dolomite is represented by isolated euhedral planar crystals or scattered patches within the fine grained matrix interval of LF-B and LF-C facies associations (Fig. 5b). Crystals are medium in size ranging between 50 and 120 μm. Dolomite occurs within micritic layers 1–2 cm thick bounded by stylolites. The analysis of major and trace elements indicate that dolomite is characterized by an excess of Ca, while trace elements are absent or present in very low concentrations (Table 2).

Interpretation:

The diagenetic features suggest that sheet cracks were formed during the initial phase of subaerial exposure (Fig. 6a–c), with cavities becoming infilled by sediments, and were successively enlarged by dissolution during prolonged subaerial exposure. The pisolitic wackestone facies, associated with the sheet cracks, are interpreted as a caliche product (cf. Assereto & Kendal 1977; Mutti 1994). A further sea-level fall resulted in the enlargement of the meteoric zone and the lowering of the transition zone between the meteoric and marine water (the mixing zone). Aggressive meteoric and mixing zone water then produced dissolution cavities in subtidal LF-A facies (Fig. 6b). The following sea-level rise resulted in the precipitation of marine cements in dissolution cavities (Fig. 6c), including crusts of radiaxial fibrous cement in the sheet cracks. This cement is not luminescent, suggesting it precipitated in oxygenating conditions and it is characterized by isotopic values consistent with Jurassic marine waters (Prokoph et al. 2008). The high concentration of Ba suggests the presence of decaying organic matter probably related to the presence of microbial mats (Table 2). Barite precipitates inorganically directly from seawater in microenvironments containing decaying organic matter and other biogenic remains (Bishop 1988; Dehairs et al. 1990; Ganeshram & Francois 2002).

After the deposition of subtidal LF-A, isopachous fibrous cement precipitated on oncoids and bioclasts. This cement is not luminescent and has a geochemical character and isotopic composition indicating precipitation from marine waters (Table 2, Fig. 7a–d). The drusy mosaic cement infilling the dissolution cavities and interparticle pores is alternating bright and non-luminescent under cathodoluminescence (Fig. 4h). It is non-ferroan, and has moderate Mn and Sr concentrations. These characteristics indicate precipitation in fluctuating oxygenated to suboxygenated conditions typical of the deeper part of the marine phreatic zone (Lohmann 1988; James & Coquette 1990). The blocky cement filling larger cavities, especially within sheet cracks, has an isotopic composition and luminescence consistent with precipitation under meteoric conditions.

Dolomite was only locally developed and occurs in association with muddy textures, stylolites and pressure solution seams. There is no evidence of former evaporites, therefore it is interpreted as a product of burial diagenesis. Burial dolomites are widely documented in the Lower Jurassic carbonates of the southern and northern Apennines (Ronchi et al. 2003; Iannace et al. 2011).

or intertidal facies

In this work, the term sedimentary cycle is used to identify commonly repeated meter-scale succession of facies associa-

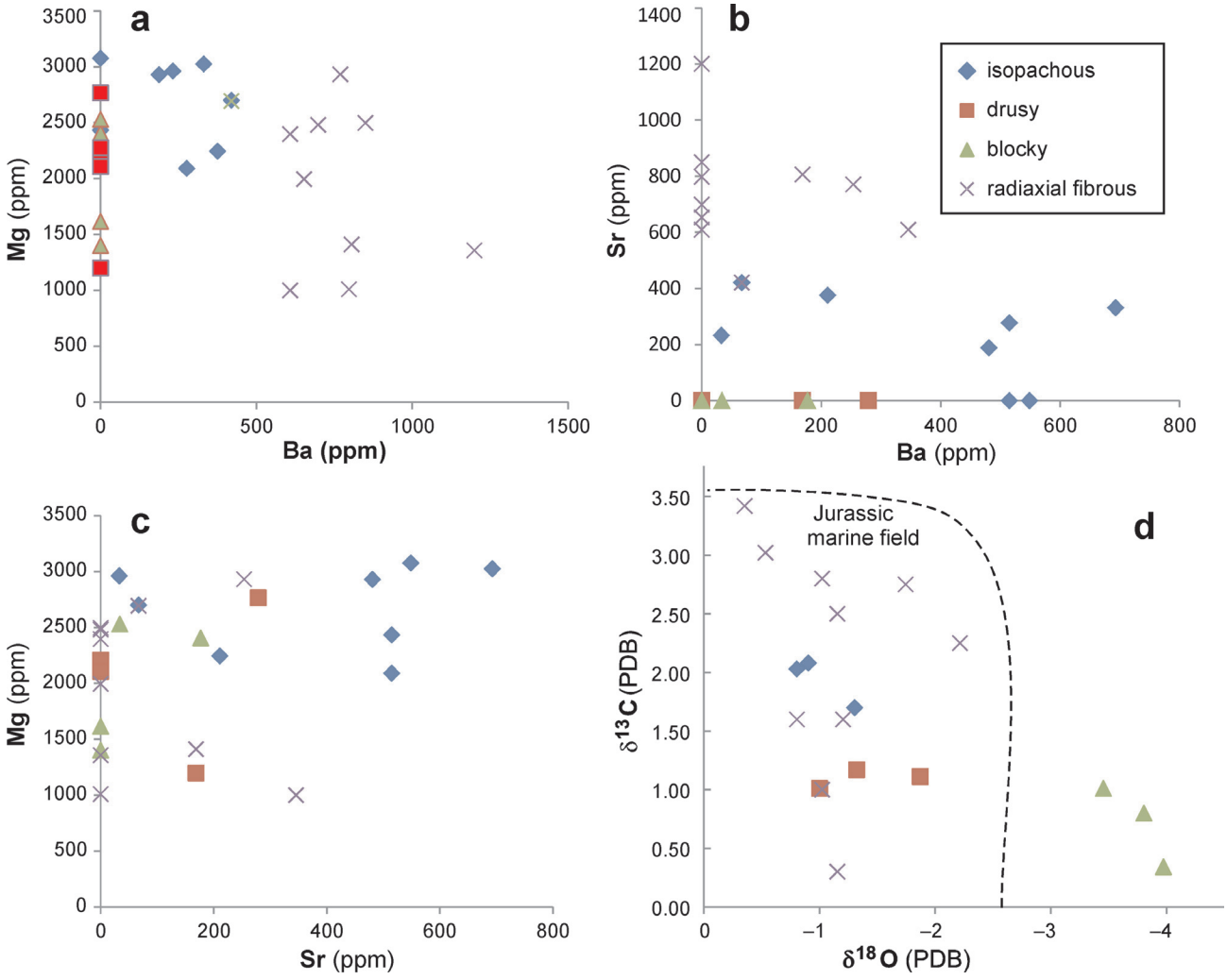

Fig. 7. Scatter diagrams of element compositions for the recognized cements. **a** — Mg vs. Ba, **b** — Sr vs. Ba, **c** — Mg vs. Sr, **d** — carbon and oxygen isotopic composition.

tion (cf. Strasser et al. 1999; Bosence et al. 2009). The cycles occur as bundles of the recognized facies associations and are bounded by a discontinuity surface. This surface is overlaid by subtidal facies of the following cycle. As observed by Bosence et al. (2000), the cycle tops are not immediately recognizable as they do not weather out on natural rock surfaces and their occurrence only becomes apparent from detailed bed-by-bed logging. Once confidently identified, the cycle tops may be followed for many hundreds of meters in the open quarry and road cut.

On the basis of the facies association stacking pattern, three types of sedimentary cycle were recognized: classic shallowing-upward cycles (Type I), symmetrical cycles (Type II), and shallowing upward cycles with non-Waltherian facies shifts (Type III) (Fig. 2).

Type I consists of a sedimentary cycle produced by a repeated meter-scale shallowing upward succession (Fig. 8A). The cycles are 0.5 to 2.5 m thick and either become finer or coarsen upward. They start with an erosion surface overlain by oncoidal floatstones to rudstones (LF-A). The basal erosional surface shows an irregular morphology, evidence of subaerial exposure, and a sharp contact with the overlying LF-A facies that may contain reworked lithoclasts and intraclasts from the underlying LF-C facies. The oncoidal floatstone to rudstone passes gradationally up into peloidal packstone alternating with cryptoalgal laminites (LF-B). Some cycles may show lenticular oncoidal beds, up to 30 cm thick laterally passing into peloidal packstone of LF-B. This cycle is bounded by LF-C facies that are connected with a period of subaerial exposure (Fig. 2). Rarely, the cycle is capped by LF-B.

Type II is 3 m thick and shows a symmetrical trend in terms of facies arrangement with peloidal packstone and cryptoalgal laminites present both at the base and in the upper portion of the cycle, separated by oncoidal floatstones to rudstones. Sheet-cracks associated with pisolitic-peloidal wackestones (LF-C) characterize the top of the cycle.

Type III cycles are between 0.5 and 1 m thick (Fig. 8b). These cycles show non-Waltherian facies shifts. An initial erosion surface is overlain by oncoidal floatstones to rudstones with skeletal fragments (LF-A), capped by desiccation cracks and pisolitic-peloidal wackestones (LF-C). In

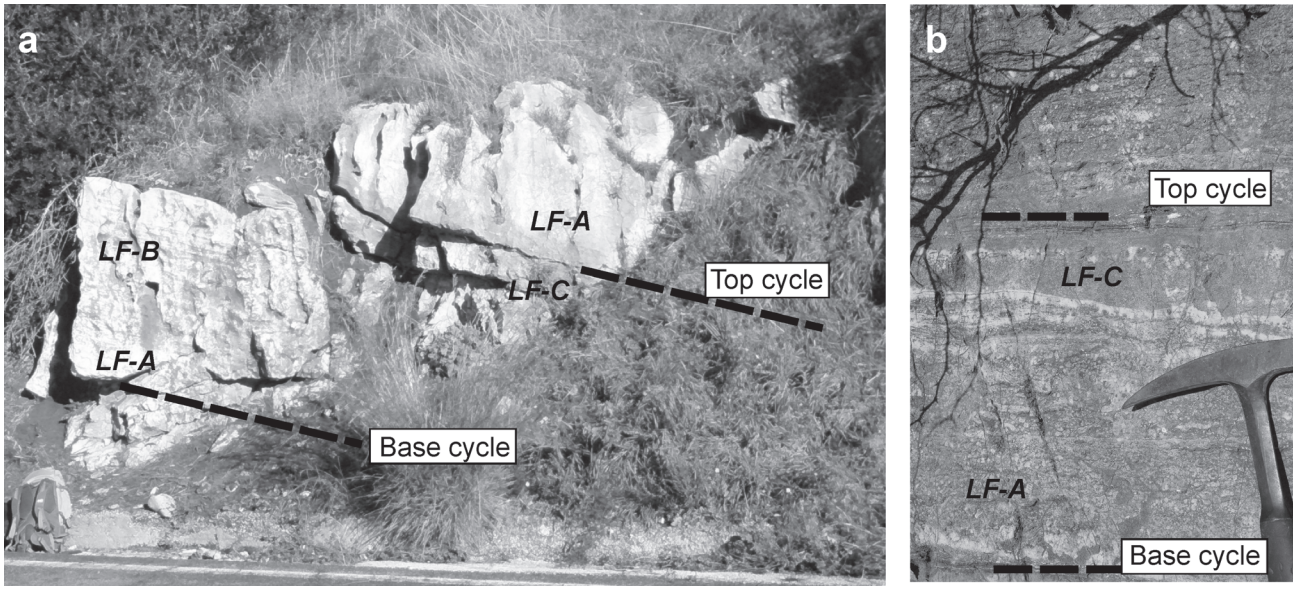

Fig. 8. a — meter-scale shallowing upward sedimentary cycle type I showing the vertical evolution from the subtidal oncoidal floatstones to rudstones facies (LF-A) to the supratidal peloidal packstone alternating with cryptoalgal laminites facies (LF-B) passing upward to the pisolitic-peloidal wackestone facies associated with sheet-cracks (LF-C). The base and the top of the cycle are characterized by an erosional surface. Dashed lines indicate the base and top of the cycle; **b** — Type III sedimentary cycle displaying basal erosion surface overlain by oncoidal floatstones to rudstones (LF-A), capped by desiccation cracks and pisolitic-peloidal wackestones (LF-C) delimited by another erosional surface corresponding to the top cycle.

Table 3: Comparison between **a**) the values estimated by Berger et al. (1989) and **b**) the peak-frequency ratios calculated in this work.

	404220	95000	47000	37000	21500	18000
a						
404220	1	4.254947	8.600426	10.92486	18.80093	22.45667
95000	0.235021	1	2.021277	2.567568	4.418605	5.277778
47000	0.116273	0.494737	1	1.27027	2.186047	2.611111
37000	0.091534	0.389474	0.787234	1	1.72093	2.055555
21500	0.053188	**0.226315**	**0.457446**	**0.581081**	**1**	**1.194444**
18000	0.04453	**0.189473**	**0.382978**	**0.486486**	**0.837209**	**1**
b						
	3.12	1.80	1.35	0.97	0.83	0.61
3.12	1	1.733333	2.311111	3.216495	3.759036	5.114754
1.80	0.576923	1	1.333333	1.85567	2.168675	2.95082
1.35	0.432692	0.75	1	1.391753	1.626506	2.213115
0.97	0.310897	0.538889	0.718519	1	1.168675	1.590164
0.83	**0.266026**	**0.461111**	**0.614815**	0.85567	**1**	**1.360656**
0.61	**0.195513**	**0.338888**	**0.451852**	0.628866	**0.73494**	**1**

this cycle the meteoric overprint is enhanced and penetrates deeply into the underlying oncoidal facies, which show dissolution features suggesting prolonged exposure.

Spectral analysis

Six main peaks have been identified in the power spectra of the investigated sections (Fig. 9): peak 1 at a frequency of 0.330995 (3.12 m), peak 2 at 0.380177 (1.8 m), peak 3 at 0.307043 (1.35 m), peak 4 at 0.158386 (0.97 m), peak 5 at 0.090113 (0.83 m) and peak 6 at 0.088033 (0.61 m). To interpret the origin of the observed high-order cyclicity, calculated ratios between peak frequencies were compared with estimated ratios for Jurassic cycles reported by Berger et al. (1989) (Table 3a). We followed the methodology of D'argenio et al. (1997, 1999) to estimate the cycle duration. This was calculated by comparing the relative ratio sets for the cycle expressed in meters (Table 3b), with the relative ratio sets of orbital parameters (Table 3a). The two ratio sets show a very good linear correlation ($r > 0.98$), suggesting that the Calcare Massiccio cycles of the investigated section had a hierarchical organization controlled by Earth's orbital perturbation.

The most prominent peaks (1.8 m and 1.35 m) are consistent with obliquity cycles, the 3.12 m peak approximates to a short eccentricity cycle (period of 95 ka), and the small peaks (0.83 m and 0.61 m) approximate to the two precession cycles (21.5 ka and 18 ka, respectively). Peak 4 (0.97 m) is not consistent with orbital cycles.

Discussion

Type I cycles correspond to the classic peritidal cycle characterized by a shallowing upward evolution and match the α cycle of Bosence et al. (2009). This cycle is the most common in the investigated section and it represents the product of regression and infilling of accommodation space. Lithofacies changes in peritidal carbonates may be caused by relative sea-level changes, but also by sediment supply, increased wave erosion or development of bedforms reducing tidal exchange (Tucker & Wright 1990). Consequently, Type I cycles may result both from autocyclic and allocyclic processes.

Type II cycles show a symmetrical facies arrangement with an intertidal facies association at the base and top separated by

a subtidal facies association. This cycle corresponds to the γ cycle of Bosence et al. (2009) and records a gradual transgressive phase followed by regression. This cycle could also result from either autocyclic or allocyclic processes.

The facies arrangement of Type III cycles shows subtidal facies directly overlain by supratidal facies. Consequently, this cycle records a marked sea-level fall resulting in subaerial exposure of subtidal facies. In this case, the cycle forms as a result of relative sea-level fall that may be caused by allocyclic processes such as eustasy or tectonic uplift.

Spectral analysis is considered an objective method for the detection of regular cyclicity in data recording oscillating parameters (Weedon 1989). In this case the sedimentary record is represented by a repetitive meter-scale succession of facies associations. In this study, spectral analysis suggests that the observed cyclic pattern of the Calcare Massiccio was controlled predominantly by orbital forcing. The vertical staking pattern of sedimentary cycles indicates a cyclical variation in cycle thickness along the section (Fig. 2). Elementary cycles are related to either the Earth's precession or obliquity signal (or a combination of both). The elementary cycles are hierarchically organized into bundles (seven groups of 1–4 elementary cycles) and the bundles into superbundles (two groups of 4 bundles), which correspond to short (~100 ka) and long (~400 ka) eccentricity signals, respectively. Consequently, the investigated portion of the Calcare Massiccio shows an accumulation rate of 1 m/30 ka, which is in agreement with the values recorded for the Tethyan Liassic carbonate platforms (see fig. 2 from Bosence et al. 2009).

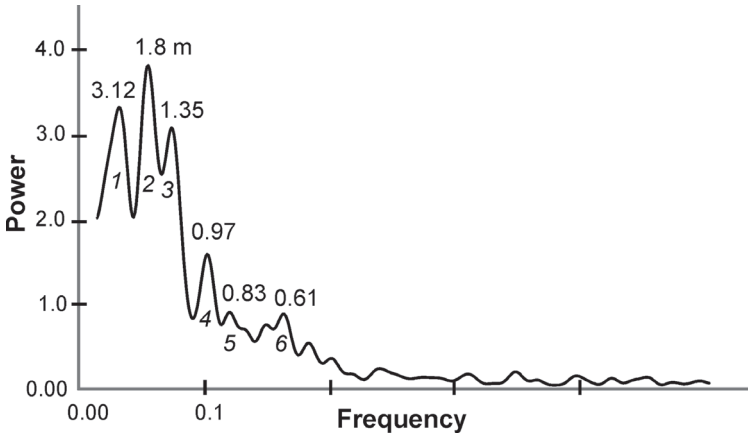

Fig. 9. Blackman-Tukey power spectrum estimation from the investigated section of Calcare Massiccio. The power spectrum indicates how much of the signal is at the recognized frequencies. The peaks show the periodicities (p = 1/f, f = frequency) recognized in the studied section.

The vertical variation of elementary cycle thickness suggests that the orbital cycles are superimposed on long-term transgressive–regressive facies trends. A transgressive facies trend is singled out on the basis of an upward increase in thickness of elementary cycles, while a regressive trend is marked by a decrease of elementary cycle thickness and an increase in restricted lagoonal deposits (LF-C and LF-B).

The carbonate cycle of the Lower Jurassic shallow-water platform in the High Atlas of Morocco has similarly been interpreted as been related to sea-level changes driven by orbital forcing (Crevello 1990, 1991).

However, the influence of autocyclic controls cannot be totally excluded because the investigated facies were deposited in a sedimentary environment, the tidal flat, where autocyclic processes are documented. Furthermore, autocyclic strata may be stacked as apparently allocyclic strata (Burgess 2006). The spectral analysis records one periodicity not consistent with orbital parameters, which may have been produced by autocyclic processes (Fig. 9).

Bosence et al. (2009) suggested a pulsed tectonic control for the creation and filling of accommodation space of some of the Calcare Massiccio peritidal cycles. However, fault activity is unlikely to be the major control on cycle repetition on extensive carbonate platforms (Tucker & Wright 1990). In this study, and in general in the Calcare Massiccio Formation, no paleoseismites were documented, which would have provided evidence for an active tectonic control during deposition.

Based on spectral analysis results, we conclude that the signal recorded in the studied succession points toward an orbital forcing control on deposition of the Calcare Massicio Formation.

High frequency sea-level fluctuations also controlled diagenetic processes in the Calcare Massiccio. Sea-level variations, by inducing changes in the water table, play a key role in exposing the peritidal cycles to the marine, mixed marine/meteoric and vadose meteoric zones (Fig. 6a,b,c). As a consequence, they are responsible for the cyclical dissolution in the vadose and mixing zone and the following precipitation of cements (cf. Mutti 1994).

Conclusion

The present paper illustrates an integrated workflow for the characterization of the Calcare Massiccio shallow-water carbonates coupling facies analysis, cyclostratigraphy and petrography.

The study highlights that the Calcare Massiccio, which developed on the structural high within the Sabina basin domain, is organized into meter-scale shallowing upward cycles bounded by subaerial exposure surfaces. The most frequent cycles show vertical evolution from a subtidal facies association (oncoid dominated) to a supratidal facies association with well-developed sheet cracks.

Spectral analysis reveals prominent peaks consistent with obliquity cycles and short eccentricity cycles, while small peaks approximate to the two procession cycles. Nevertheless, one of the recorded peaks is not consistent with any orbital cyclicity.

We conclude that, in the Calcare Massiccio, a tectonic control on sedimentary cycle development cannot be disregarded, but the signal recorded by the sedimentary succession points toward a significant control by orbital forcing.

The diagenetic characteristics of Calcare Massiccio are linked to high frequency sea-level fluctuations, which produced dissolution during sea-level fall and cement precipitation during following sea-level rise as illustrated by marine cements precipitated inside sheet cracks developed on top of the cycles.

Acknowledgments: Financial support from MIUR (PRIN 2010-11 Research Grant 20107ESMX9_001 and Sapienza Ateneo Project 2014) are gratefully acknowledged. Criticism and comments by František Vaček and an anonymous reviewer greatly improved the manuscript. Comments by Editor Jindřich Hladil are much appreciated. The authors would like to thank Flavio Jadoul for the cathodoluminescence analysis. Discussions in the field with Alessandro Lanfranchi were very useful. Mariano Parente is thanked for assistance with the Strontium Stratigraphy. Useful discussions with Dan Bosence, Fotini Pomoni-Papaioannou, Sabrina Amodio and Julien Michel are much appreciated. Marcello Serracino is thanked for the assistance with EDS-WDS analyses. We thank James Hodson (RPS Energy) for comments and English review.

References

Assereto R.L.A.M. & Kendall St.C. 1977: Nature, origin and classification of peritidal tepee structures and related breccias. *Sedimentology* 24, 153–210.

Barattolo F. & Bigozzi A. 1996: Dasycladaleans and depositional environments of the Upper Triassic–Liassic carbonate platform of the Gran Sasso (Central Apennines, Italy). *Facies* 35, 163–208.

Berger A.F., Loutre M.F. & Dehant V. 1989: Influence of the changing lunar orbit on the astronomical frequencies of the Pre-Quaternary insolation patterns. *Paleoceanography* 4, 555–564.

Bigozzi A. 1990: Cyclic stratigraphy of the Upper Triassic–Lower Liassic sequence of Corno Grande (Central Apennines). *Mém. Soc. Geol. Ital.* 45, 709–721.

Billi A., Valle A., Brilli M., Faccenna C. & Funiciello R. 2007: Fracture-controlled fluid circulation and dissolutional weathering in sinkhole-prone carbonate rocks from central Italy. *J. Struct. Geol.* 29, 385-395.

Bishop J.K.B. 1988: The barite–opal–organic carbon association in oceanic particulate matter. *Nature* 331, 341–343.

Blackman R.B. & Tuckey S.W. 1958: The measurement of power spectra. *Dover Publications*, New York, 1–190.

Bosence D.W.J., Wood J., Rose E.P.F. & Qing H. 2000: Low and high frequency sea-level changes control peritidal carbonate cycles, facies and dolomitization in the Rock of Gibraltar (Early Jurassic, Iberian Peninsula). *J. Geol. Soc. London* 157, 61–74.

Bosence D., Procter E., Aurell M., Kahla A.B., Marcelle B.F., Casaglia F., Cirilli S., Mehdie M., Nieto L., Rey J., Scherreiks R., Soussi M. & Waltham D. 2009: A dominant tectonic signal in high-frequency, peritidal carbonate cycles? A regional analysis of liassic platforms from western Tethys. *J. Sed. Res.* 79, 389–415.

Burgess P.M. 2001: Modelling carbonate sequence development without relative sealevel oscillations. *Geology* 29, 1127–1130.

Burgess P.M. 2006: The signal and the noise: forward modelling of allocyclic and autocyclic processes influencing peritidal carbonate stacking patterns. *J. Sed. Res.* 76, 962–977.

Carminati E. & Doglioni C. 2005: Mediterranean tectonics. In: Selley R., Cocks R. & Plimer I. (Eds): Encyclopedia of Geology. *Elsevier*, 135–146.

Carminati E., Lustrino M., Cuffaro M. & Doglioni C. 2010: Tectonics, magmatism and geodynamics of Italy: What we know and what we imagine. *J. Virtual Explorer* 36, 9, 1–64.

Carminati E., Corda L., Mariotti G., Scifoni A. & Trippetta F. 2013: Mesozoic syn- and postrifting evolution of the Central Apennines, Italy: The role of Triassic evaporates. *J. Geology* 121, 4, 327–354.

Carozzi A.V. 1957: Contribution a l'étude des propriétés géométriques des oolithes. L'exemple du Grand Lac Salé, Utah, USA. *Bull. Inst. Natl. Genevois* 58, 3–52.

Centamore E., Chiocchini G., Deiana A., Micarelli U. & Pieruccini M. 1971: Contribution to the knowledge of the Jurassic of the Umbria-Marche Apeninnes. [Contributo alla conoscenza del Giurassico dell'Appennino umbro-marchigiano.] *Studi Geol. Camerti* 1, 7–89 (in Italian).

Choquette P.W. & Pray L.C. 1970: Geologic nomenclature and classification of porosity in sedimentary carbonates. *AAPG Bull.* 54, 207–250.

Colacicchi R., Passeri L. & Pialli G. 1975: Evidences of tidal environment deposition in the Calcare Massiccio Formation (Central Apennines-Lower Lias). In: Ginsburg R. (Ed.): Tidal deposits, a casebook of recent examples and fossil counterparts. Section IV. *Springer-Verlag*, Berlin, 345–353.

Cosentino D., Cipollari P. & Pasquali V. 2004: The Jurassic pelagic carbonate platform of the Cornicolani Mts. (Latium, central Italy). In: Pasquarè G. & Venturini C. (Eds.): Mapping geology of Italy. *APAT-SELCA*, *IGC,* Florence, 177–184.

Crevello P. 1990: Stratigraphic evolution of Lower Jurassic carbonate platforms: record of rift tectonics and eustasy, central and eastern High Atlas, Morocco. *Ph.D. Dissertation, Colorado School of Mines*, Golden, Colorado, 1–456.

Crevello P. 1991: High frequency carbonate cycles and stacking patterns: interplay of orbital forcing and subsidence on Lower Jurassic rift platforms, High Atlas, Morocco. In: Franseen E.K., Watney W.L., Kendall C.G.St.C. & Ross W. (Eds.): Sedimentary modelling: computer simulations and methods for improved parameter definition. *Kansas Geol. Surv., Bull.* 223, 207–230.

D'Argenio B., Ferreri V. & Amodio S. 2011: Eustatic cycles and tectonics in the Cretaceous shallow Tethys, Central-Southern Apennines. *Ital. J. Geosci.* 130, 119–127.

D'Argenio B., Ferreri V., Amodio S. & Pelosi N. 1997: Hierarchy of high-frequency orbital cycles in Cretaceous carbonate platform strata. *Sed. Geol.* 113, 169–193.

D'Argenio B., Ferreri V., Raspini A., Amodio S. & Buonocunto F.P. 1999: Cyclostratigraphy of a carbonate platform as a tool for high-precision correlation. *Tectonophysics* 315, 357–384.

Damiani A.V., Chiocchini M. Colacicchi R., Mariotti G., Parotto M., Passeri L. & Praturlon A. 1992: Lithostratigraphic elements for a summary of the Meso-Cenozoic carbonate facies of the Central Apeninnes. [Elementi litostratigrafici per una sintesi delle facies carbonatiche meso-cenozoiche dell'Appennino centrale.] In: Tozzi M., Cavinato G.P. & Parotto M. (Eds.): Preliminary studies on the acquisition data for the CROP11 Civitavecchia-Vasto profile. [Studi preliminari all'acquisizione dati del profilo CROP 11 Civitavecchia–Vasto.] *Studi Geol. Camerti*, vol. spec. 1991/2, 187–213 (in Italian).

Dehairs F., Goeyens L., Stroobants N., Bernard P., Goyet C., Poisson A. & Chesselet R. 1990: On the suspended barite and the oxygen minimum in the Southern Ocean. *Global Biogeochemical Cycles* 4, 85–102.

Doglioni C. 1991: A proposal of kinematic modelling for W-dipping subductions — possible applications to the Tyrrhenian–Apennines system. *Terra Nova* 3, 423–434.

Dunham R.J. 1962: Classification of carbonate rocks according to depositional texture. In: Ham W.E. (Ed.): Classification of carbonate rocks. *Amer. Assoc. Petrol. Geol. Mem.* 1, 108–121.

Dupraz C. & Strasser A. 1999: Microbialites and micro-encrusters in shallow coral bioherms (Middle to Late Oxfordian, Swiss Jura Mountains). *Facies* 40, 101–130.

Elliott G.F. 1956: Further records of fossil calcareous algae from the Middle East. *Micropaleontology* 2, 327–334.

Embry A.F. & Klovan J.E. 1971: A Late Devonian reef tract on northeastern Banks Island, Norhwest Territories. *Canad. Petrol. Geol. Bull.* 19, 730–781.

Galluzzo F. & Santantonio M. 2002: The Sabina Plateau: a new element in the Mesozoic palaeogeography of Central Apennines. *Boll. Soc. Geol. Ital.* 1, 561–588.

Ganeshram R. & Francois R. 2002: New insights into the mechanism of barite formation in seawater and implications for paleoproductivity reconstruction. *EOS Trans. Amer. Geophys. Union* 83, Ocean Science Meeting Supplement, Abstract OS21L-11.

Ginsburg R.N. 1971: Landward movement of carbonate mud — new model for regressive cycles in carbonates. *Amer. Assoc. Petrol. Geol. Bull.* 55, 340.

Gueguen E., Doglioni C. & Fernandez M. 1998: On the post-25 Ma geodynamic evolution of the Western Mediterranean. *Tectonophysics* 298, 259–269.

Hardie L.A. 1986: Stratigraphic models for carbonate tidal flat deposition. In: Hardie L.A. & Shinn E.A. (Eds.): Carbonate depositional environments, modern and ancient. Part 3. Tidal flats. *Colorado School of Mines, Quarterly* 81, 59–73.

Iannace A., Capuano M. & Galluccio L. 2011: "Dolomites and dolomites" in Mesozoic platform carbonates of the Southern Apennines: geometric distribution, petrography and geochemistry. *Palaeogeogr. Palaeoclimatol. Palaeoecol.* 310, 324–339.

James N.P. & Coquette P. 1990: Limestones — the meteoric diagenetic environment. In: McIlreath I.A. & Morrow D.A. (Eds.): Diagenesis. *Geoscience Canada Reprint Series* 4, 35–73.

Lohmann K.C. 1988: Geochemical patterns of meteoric diagenetic systems and their application to studies of paleokarst. In: James N.P. & Choquette P.W. (Eds.): Paleokarst. *Springer–Verlag*, New York, 58–80.

Lukasik J. & Simo J.A. (Toni) 2008: Controls on development of Phanerozoic carbonate platforms and reefs — introduction and synthesis. In: Lukasik J. & Simo J.A. (Toni) (Eds): Controls on carbonate platform and reef development. *SEPM Spec. Publ.* 89, 5–12.

Mutti M. 1994: Association of tepees and paleokarst in the Ladinian Calcare Rosso (Southern Alps, Italy). *Sedimentology* 41, 621–641.

Paillard D., Labeyrie L. & Yiou P. 1996: Macintosh program performs time-series analysis. *EOS Trans. Amer. Geophys. Union* 77, 379.

Passeri L. & Venturi F. 2005: Timing and causes of drowning of the Calcare Massiccio platform in Northern Apennines. *Boll. Soc. Geol. Ital.* 124, 1, 247–258.

Pialli G. 1971: Co-tidal flat facies in the Calcare Massiccio of the Umbria-Marche Apeninnes. [Facies di piana cotidale nel Calcare Massiccio dell'Appennino Umbro-Marchigiano.] *Boll. Soc. Geol. Ital.* 90, 481–507 (in Italian).

Pomoni-Papaioannou F. & Kostopoulou V. 2008: Microfacies and cycle stacking pattern in Liassic peritidal carbonate platform strata, Gavrovo-Tripolitza platform, Peloponnesus, Greece. *Facies* 54, 417–431.

Pratt B.R., James N.P. & Cowan C.A. 1992: Peritidal carbonates. In: Walker R.G. & James N.P. (Eds.): Facies models: Response to sea level change. *Geol. Assoc. Canada*, 303–322.

Prokoph A., Shields G.A. & Veizer J. 2008: Compilation and time-series analysis of a marine carbonate $\delta^{18}O$, $\delta^{13}C$, $^{87}Sr/^{86}Sr$ and $\delta^{34}S$ database through Earth history. *Earth Sci. Rev.* 87, 113–133.

Radoičić R. 1959: Some problematic microfossils from the Dinarian Cretaceous. *Bull. Serv. Géol. Géophys. RP Serbie* 17, 87–92.

Ronchi P., Casaglia F. & Ceriani A. 2003: The multiphase dolomitization of the Liassic Calcare Massiccio and Corniola succession (Montagna dei Fiori, Northern Apennines, Italy). *Boll. Soc. Geol. Ital.* 122, 157–172.

Santantonio M. 1993: Facies associations and evolution of pelagic carbonate platform/basin systems: examples from the Italian Jurassic. *Sedimentology* 40, 1039–1067.

Schmid D.U. & Leinfelder R.R. 1996: The Jurassic *Lithocodium aggregatum–Troglotella incrustans* foraminiferal consortium. *Palaeontology* 39, 21–52.

Schwarzacher W. 1993: Cyclostratigraphy and the Milankovitch Theory. *Developments in Sedimentology* 52, *Elsevier*, Amsterdam, 1–225.

Strasser A. 1994: Milankovitch cyclicity and high-resolution sequence stratigraphy in lagoonal-peritidal carbonates (Upper Tithonian–Lower Berriasian, French Jura Mountains). In: De Boer P.L. & Smith D.G. (Eds): Orbital forcing and cyclic sequences. *IAS Spec. Publ.* 19, *John Wiley & Sons*, 285–301.

Strasser A. & Védrine S. 2009: Controls on facies mosaics of carbonate platforms: a case study from the Oxfordian of the Swiss Jura. In: Swart P.K., Eberli G.P. & McKenzie J.A. (Eds.): Perspectives in carbonate geology. *IAS Spec. Publ.* 41, *Wiley–Blackwell*, 199–213.

Strasser A., Hilgen F.J. & Heckel P.H. 2006: Cyclostratigraphy — Concepts, definitions, and applications. *Newslett. Stratigr.* 42, 75–114.

Strasser A., Pittet B., Hillgärtner H. & Pasquier J.B. 1999: Depositional sequences in shallow carbonate-dominated sedimentary systems: Concepts for a high-resolution analysis. *Sed. Geol.* 128, 201–221.

Tucker M.E. & Wright V.P. 1990: Carbonate sedimentology. *Blackwell Scientific Publications*, Oxford, 1–482.

Védrine S., Strasser A. & Hug W. 2007: Oncoid growth and distribution controlled by sea-level fluctuations and climate (Late Oxfordian, Swiss Jura Mountains). *Facies* 53, 535–552.

Weedon G. 1989: The detection and illustration of regular sedimentary cycles using Walsh power sectra and filtering, with samples from the Lias of Switzerland. *J. Geol. Soc.* 146, 133–144.

Weedon G. 2003: Time-series analysis and cyclostratigraphy. Examining stratigraphic record of environmental cycles. *Cambridge University Press*, New York, 1–259.

Wright V.P. & Burgess P.M. 2005: The carbonate factory continuum, facies mosaics and microfacies: an appraisal of some of the key concepts underpinning carbonate sedimentology. *Facies* 51, 17–23.